Hairstyle Construction from Raw Surface Data

Gerrit Sobottka, Michael Kusak, Andreas Weber
Institute of Computer Science II, University of Bonn, Germany
{sobottka, kusak,weber}@cs.uni-bonn.de

Abstract

We present a novel approach to the problem of hairstyle construction from raw surface data such as the ones obtained from surface scans. Our approach is based on a shape matching algorithm that fits individual hair fibers into a given volume according to a set of boundary conditions and additional hair density information. Our method employs a mechanical rod model based on the special theory of Cosserat rods. Such models can efficiently be used to simulate the deformation of individual fibers in subsequent manipulation steps.

Keywords—**Hair modeling, hairstyle construction, hair volume, surface data, optimization, fibers, Cosserat rods**

1 Introduction

Generating realistic looking hairstyles is an unresolved problem in the realm of computer graphics. Standard approaches still require a high degree of manual effort because the main flow directions must be given in terms of guide hairs. Whereas the problem of reconstructing local hair geometries out of sequences of photographs has been addressed recently, the problem of hair style generation from raw surface data has not been incorporated in existing approaches so far. Such surface data can be obtained from scans of sculptures. The boundaries of the hairstyle are defined by the scalp as well as the hair volume surface. A possibility to construct plausible hairstyles considering the volume boundaries is of great interest for different purposes, e.g. in the context of virtual heritage projects.

Our contribution: We present a new approach to the problem of constructing realistic looking hairstyles from raw surface data. In contrast to other approaches our algorithm is automated, yet fully customizable by the user through the specification of only a handful of parameters. No manual interactions are required. To model the hair fibers we employ a mechanical model based on the special theory of Cosserat rods. Our approach is thus physical and allows us to estimate the magnitude of forces occurring inside the hair volume.

2 Related Work

In the last few years several approaches to the hairstyle generation problem have been introduced. Lee et al. [10] presented a system for hairstyle creation which allows interactive manipulation of computer generated hairstyles using a motion tracking device. Hadap and Thalmann [7] presented a method that models the hair geometry as ideal fluid flow. Sources are placed along the scalp surface to prevent streamlines from penetrating the object boundaries. However, even high source densities cannot guarantee a penetration free hairstyle. This is closely related to our approach as we use linear approximations of the object boundaries on rectilinear grids to tackle the penetration problem. Moreover, this approach alone cannot account for other geometries than soft curves with small curvature. In [17] Yu pursues a similar approach by exploiting the analogy between smooth vector fields and hair flow. Procedurally generated vector field primitives are superimposed to obtain complex hairstyles. In [16] Xu and Yang presented a modeling tool based on a cluster hair model. Simple operations are used for the interactive creation and manipulation of hair clusters. In the same spirit, Kim and Neumann [9] present a so called multi resolution hair modelling system wherein hair is modeled on a per-cluster basis. The full hairstyle in obtained from a sequence of copy and paste, curling and moving operations of hair primitives as well as user driven refinements of individual clusters to add more detail to the hairstyle. Recently, Choe and Ko [4] presented a hair styling tool that is based on a pseudo-physical approach. Similar to ours, it uses force as well as density fields to approximate the impact of gravity and hair-hair interaction, respectively.

The aforementioned approaches have in common that hairstyles are manually modeled with interactive tools. The computer vision approach, on the other hand, which primarily aims at the reconstruction of hairstyles from a set of photos has recently gained increased attention.

Haider and Kaneko [8] proposed an algorithm for hair volume reconstruction from a set of video captured images. A hairless 3D head model obtained from CT scans is used for the registration of camera parameters. After segmentation of the hair region in the images and the registration of the camera positions a three dimensional hair volume is computed. The extracted hair texture is then mapped to the model. This is in fact a pure volume based model because no hair fibers are generated. Recently, Paris et al. [13] proposed an algorithm for hair geometry reconstruction from a set of images taken under variable lighting conditions. Different filter operations are applied to these images to determine the orientation of each pixel. From these data the full hairstyle is computed according to the visual hull and additional information like camera positions. The most impressing results, however, are obtained with the image based approach of Wei et al. [15]. Only a set of images taken under uncontrolled lighting conditions are needed. The orientation of each hair segment is triangulated with orientation information from multiple views. The shape of the skull is approximated by an offset surface of the visual hull.

The reconstruction with these approaches requires that local orientation information are given or can at least be recon-

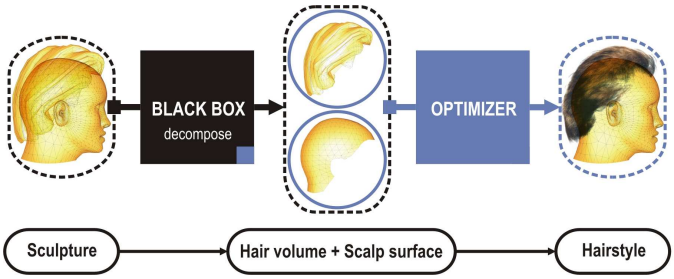

Fig. 1. The input for our model is given by the scalp and the hair volume surface. The extraction of the surfaces from sculpture scans are beyond the scope of this paper and left as a black box process.

structed. Thus, these algorithms cannot be used for sculpture scans, by which only the boundary corresponding to the visual hull is given.

3 Outline of the Algorithm

Our algorithm takes as input the scalp surface $\mathcal{S}_S$, and, in addition, the boundary $\mathcal{S}_H$ of an associated hair volume, cf. Fig. 1. Starting from a sculpture scan the basic task is to decompose the surface of the sculpture into the required input data. One possibility to solve this difficult problem is to generate a scalp surface as an offset surface from the hair volume boundary. However, this is a rather approximate solution at best. A more promising approach is to search for a similar hair-less head model in a large data set of head models and to subtract it from the sculpture scan to obtain the hair volume. This approach is similar to the *morphable head models* of Blanz and Vetter [2]. We have not employed a fully automated method for this preprocessing step. For our examples we have generated some examples semi-manually. This pre-processing step can be taken as a black box for the following algorithm, which is the main topic of this paper.

Given the boundaries defined by the scalp as well as the hair volume surface we solve an optimization problem in order to find optimal terminal force-torque pairs which deform the fibers to an "optimal" configuration according to their distances from the boundaries as well as local hair density information. Technically, we solve an unconstrained optimization problem by formulating various "contraints" as "soft constraints". Since our starting basis is an empty volume we first generate a set of *pre-guides* which coarsely sample the main flow directions for *principal guide* generation. After the optimization process we compute for each principal guide a hair strand (wisp) employing a simple strand generator. We refer to the volume encapsulated by the scalp surface and the hair volume surface as *acceptable region*. The transition between the acceptable region and the non-acceptable or forbidden region is smooth.

In the following we will discuss in detail the components of our system needed to generate hairstyles from raw surface data.

3.1 Special Theory of Cosserat Rods

To simulate a single hair fiber we employ a mechanical rod model based on the special theory of Cosserat rods [1]. Let $\mathbf{r}(s) : [a, b] \in \mathbb{R} \mapsto \mathbb{R}^3$ be a smooth space curve of length L describing the centerline of a hair fiber. Further, let $\{\mathbf{d}_i(s)\}$ be a set of orthogonal directors furnishing the space curve such that $\mathbf{d}_1$, $\mathbf{d}_2$ span the cross section plane and $\mathbf{d}_3 = \mathbf{r}'$ is tangent to space curve, where $(\cdot)'$ denotes the derivative with respect to arc length. The special theory of Cosserat rods [1] used herein describes the deformation of a long thin elastic rod subject to external loads. Since we are only interested in the equilibrium configurations the static equations governing this state are given as

$$\mathbf{n}' + \mathbf{f} = \mathbf{0}, \tag{1}$$

$$\mathbf{m}' + \mathbf{r}' \times \mathbf{n} + \mathbf{g} = \mathbf{0}, \tag{2}$$

where $\mathbf{n}$ and $\mathbf{m}$ are the contact force and contact couple at the cross sectional area, respectively. $\mathbf{f}$ and $\mathbf{g}$ are the external forces and moments acting on the rod. Further, we have the kinematic relation

$$\mathbf{d}_i' = \mathbf{u} \times \mathbf{d}_i. \tag{3}$$

Here, $\mathbf{u}$ indicates the twist vector and expresses the local bending and twist about the three directors. The relation between local deformations expressed by the twist vector and the material properties is given by suitable constitutive laws. For our purposes we assume the rod to be hyper-elastic, unshearable, and inextensible. Hence, the constitutive relation takes the simple form $\mathbf{m} = \mathbf{C} \cdot (\mathbf{u} - \hat{\mathbf{u}})$, where $\mathbf{C}$ is a diagonal matrix describing the material's resistance against bending and twist about the three axes:

$$\mathbf{C} = \begin{pmatrix} EI_1 & 0 & 0 \\ 0 & EI_2 & 0 \\ 0 & 0 & GA \end{pmatrix}. \tag{4}$$

Here, we can work with authentic material properties of human hair of $E = 3.89 \cdot 10^{10}$ and $G = 0.89 \cdot 10^{10}\,\mathrm{dynes/cm}$ for Young's modulus and the shear modulus, respectively. The vector $\hat{\mathbf{u}}$ describes the default twist of the rod and $I_{1,2}$ are the principal moments of inertia of the cross section A ($\approx 1.5 \cdot 10^{-5}\,\mathrm{cm}^2$).

Since the filaments are clamped at the scalp and can freely move at the other end, we obtain the following boundary conditions: $\mathbf{r}(0) = \mathbf{r}_0$, $\mathbf{d}_1(0) = \mathbf{d}_{10}$, $\mathbf{d}_2(0) = \mathbf{d}_{20}$, $\mathbf{f}(L) = \mathbf{f}_L$, and $\mathbf{t}(L) = \mathbf{t}_L$, where $\mathbf{f}_L$ and $\mathbf{t}_L$ are the external force and torque acting at $s = L$.

Thus, we have to solve boundary value problems for a coupled system of ordinary differential equations. Standard BVP solvers are often based on shooting techniques which usually perform at slow convergence rates. In [11] a solution method for this particular type of boundary value problem based on the Kirchhoff kinetic analogy is proposed. In [14] a simple energy minimization scheme is proposed that is also capable of handling intermediate boundary conditions. In [12] Pai introduces a rather approximate solution scheme

by decoupling the kinematic relations from the balance laws. Unfortunately, this approach treats forces and torques with respect to the local systems which transforms each force into a follower load, a problem which is discussed in more detail in [14]. In order to enable the incorporation of different solution schemes we parameterized our system with different solution schemes for BVPs.

3.2 Boundary Representation

Another central problem we have to deal with is the efficient representation of the scalp as well as the hair volume surface, such that hairs are prevented from occupying the forbidden area outside the boundaries. For this purpose, we compute for the surfaces $\mathcal{S}_S$ and $\mathcal{S}_H$ an implicit linear approximation or distance field Φ_S which is a scalar mapping $\Phi_S : \mathbb{R}^3 \rightarrow \mathbb{R}$ such that

$$\Phi_S(\mathbf{x}) := \min_{\mathbf{q} \in \mathcal{S}} \{|\mathbf{x} - \mathbf{q}|\}, \, \forall \mathbf{x} \in \mathbb{R}^3. \tag{5}$$

We decided to use simple a rectilinear grid because of improved performance over octree encodings; notice that the increase in memory costs is negligible for our applications. Since we do not assume that the mesh obtained in the preprocessing steps is closed, we only compute a distance envelope of a predefined thickness. This is done using the method of characteristics [3]. For each feature of the underlying meshes the corresponding Voronoi region is computed. We then calculate the distances of all grid points within a Voronoi region to the corresponding feature using a scan conversion algorithm. It is possible to sign the distances by taking into account the direction of the normal of each triangle. The normals of the triangles indicate the "exterior" if the underlying mesh is oriented. The signs of the distances are then chosen according to the signs of the scalar products of the point's local position vectors and the normals of the triangles to which the closest feature belongs. For a given point the distance to a surface can be computed by means of a trilinear interpolation over the distances at the eight corner points of the corresponding cell.

3.3 Hair Distribution and Growth Directions

In order to allow for an uniform distribution of the hair pores on the scalp surface $\mathcal{S}_S$ we parameterize it using a conformal mapping $C : \mathbb{R}^3 \mapsto \mathbb{R}^2$ such that the surface is projected onto the plane by using a Floater parameterization [5], which guarantees a one-to-one mapping. The parameter domain is mapped onto the unit circle. We then compute a homogeneous point distribution and map it back onto the corresponding triangles by using the barycentric coordinates of the points. In the examples we use authentic density values of 200 hairs per cm. After the point distribution we cluster points by computing a covering with circles of the 2D domain. The center of each cluster is taken as base position for the guides. Since the circles are allowed to overlap we randomly associate affected points to one of the guides to which the region belongs. This prevents sharp-edged base areas of the final clusters. Simple shape distortion minimizing schemes like the above cannot avoid distortion of the texture in general. We found that carefully chosen parameters can minimize such effects for meshes with simple topologies like the scalp surface which resembles a hemisphere. The remaining distortion is advantageous in the sense that it deforms circular base areas into more elliptical ones.

The hair density, the growth directions, and the hair length distributions are encoded in a texture bitmap by means of grey values. Unfortunately, little empirical facts about the real growth direction distribution on the scalp can be found in the literature. From our own observations we know that hair in the temporal as well as the occipital region of the head growth in tangential direction rather than normal to the surface. This is an important fact to consider as it allows for more realistic looking hairstyles, as is demonstrated by our results.

The guides are deformed according to the scheme that is described in the following section.

3.4 Guide Generation

With the rod model defined above and the definition of the linear approximation of the boundary surfaces at hand we can now develop an algorithm to keep the fibers inside the acceptable region and follow the flow defined by the pre-guides. We define as $\eta_L = \{\mathbf{f}_L, \mathbf{t}_L\}$ the terminal end load acting on a fiber at $s = L$. In particular, we seek a terminal end load η_L^* consisting of a force and a torque that minimizes an objective function which we will describe next. Thus, our optimization problem is a six-dimensional one.

One might be wondering why a terminal force-torque pair is sufficient? However, the reason is rather obvious: using a terminal force-torque pair allows one to model arbitrary configurations including helices. A terminal force alone can only generate arcs whereas the additional incorporation of torques extends the variety of possible shapes. In principle, it is also possible to use intermediate loads but this only increases the dimension of the underlying optimization problem. Direct control of bending angles as was proposed by [4] does not guarantee a continuous curve as is the case when we use a mechanical rod model.

Pre-Guide Generation: The pre-guides are generated according to the following scheme: First the base points for the pre-guides are distributed with a low density of 1 fiber per cm or less, cf. Sect. 3.3. Then we rotate the pre-guides into the direction of the corresponding growth normals. After the pre-guides took their initial positions we iteratively increase a terminal end load until the extremities immerses into the hair volume by a predefined depth. The force has a direction normal to the rod's initial axes and lies within the plane defined by the normal of the triangle and the corresponding rotated normal obtained from the growth direction distribution texture. The immersion depth is chosen such that the frontal hairs are close to the hair volume surface and increases according to the geodetic height of the base points. Thus, lower guides generate the lower hair layers of the style. The maximum possible depth are obtained by superposition of the distance fields for the scalp surface and the hair volume surface, respectively.

Principal Guide Generation: The objective function to be minimized is a weighted sum of n terms, each of which controls a certain aspect of the underlying problem. This function is given by

$$\min f(\eta) = \sum w_i \cdot \mathcal{F}_i, \tag{6}$$

where $\mathcal{F}_i : \mathbb{R}^3 \mapsto \mathbb{R}$ are scalar valued functions and $w_i \in \mathbb{R}$ are the respective weights, with $\sum w_i = 1$.

The first term $\mathcal{F}_1$ accounts for the directional correspondence of the current guide to its adjacent pre-guides and is given as

$$\mathcal{F}_1 = \int_0^1 \left(1 - \left\langle \frac{\mathbf{r}'_G}{|\mathbf{r}'_G|}, \frac{\mathbf{r}'_C}{|\mathbf{r}'_C|} \right\rangle\right) \mathrm{d}s. \tag{7}$$

This correspondence is measured in terms of the cosine of the angle between the local tangents of the guide and the current fiber at the positions $\mathbf{r}_G(s)$ and $\mathbf{r}_C(s)$, respectively. The function, thus obeys $(1 - \cos\varphi)$. That is, if the local directions are parallel, then the function evaluates to zero, if they are orthogonal to one and the function takes its highest value if they are antiparallel. This function is evaluated for a variable number of pre-guides in the vicinity of the current guide. We found that three pre-guides are sufficient. The contribution of each pre-guide is weighted according to its distance from the guide on the scalp. This allows for more smooth transitions. Please note, that $\mathbf{r}'(s) = \mathbf{d}_3(s)$.

The second term $\mathcal{F}_2$ accounts for the similarity of the current guide to the pre-guides. It is defined as

$$\mathcal{F}_2 = \left[\int_0^1 \left(\Delta\mathbf{u}^2\right) \mathrm{d}s\right]^{\frac{1}{2}}. \tag{8}$$

The local curvature and torsion is the used measure for the similarity of two curves. These quantities are given by the twist vector $\mathbf{u}$, cf. Sec. 3.1. The vector $\Delta\mathbf{u} = \mathbf{u}_G - \mathbf{u}_C$ describes the twist difference between the guide and the current curve. Note that since the curves need not be of the same length we use the normalized curves, thus $s \in [0, 1]$.

The third term $\mathcal{F}_3$ deals with the problem of boundary penetration of individual fibers and is given as

$$\mathcal{F}_3 = \begin{cases} |d|, & \text{if } d < 0 \\ c_d + |d|, & \text{if } d > 0 \end{cases}. \tag{9}$$

As has been mentioned before the boundary is formed by the scalp and the hair surface, respectively. We calculate the distance of each point to the boundaries using the corresponding distance fields, cf. Sect. 3.2. As can be seen in the equation we punish harder if a fiber is outside the boundaries by adding a constant value of c_d. The function is applied for both surfaces, the scalp and the hair volume.

The contributions of the above terms can conveniently be controlled by the weighting parameters w_i, e.g., the higher the contribution of the similarity controlling term is the better the match of the principal guides to the shape of the corresponding pre-guides is.

For each guide we start the optimization process from a straight configuration ($\hat{\mathbf{u}} = \mathbf{0}$) pointing in the direction of the corresponding growth normal, cf. Sect. 3.3.

3.5 Using Local Density Information

To account for hair-hair interactions and to obtain a more homogeneous fiber distribution throughout the acceptable hair region we also incorporate local density information. For this purpose, we iteratively generate a density field that describes the approximate local hair density at each point of the acceptable hair region. The density field is encoded on a rectilinear grid. If the local density in the region that a guide and its corresponding strand will presumably occupy is larger than a predefined threshold, then we add a high surcharge to the energy value. If a principal guide takes its final configuration, then the densities within a cylindrical region around the guide are added to the voxels occupied by it. This cylindrical region will later be filled with hair by a simple strand generator.

Here, we discuss two different density models:

- **Binary occupancy model (BOM)**: In this model the voxels occupied by a full strand are assigned the value 1. The corresponding grid must have a high resolution such that the region filled by a single segment remains small. We incorporate this model into the objective function by adding a fourth term:

  $$\mathcal{F}_4^{BOM} = c_{BOM} \cdot \sum \delta(\mathbf{s}_i). \tag{10}$$

  The function δ evaluates to 1 if segment $\mathbf{s}_i$ intersects an occupied voxel, 0 otherwise. That is, for each segment of a guide that penetrates an occupied cell we add a value of c_{BOM}. To determine the occupancy we employ a simple voxelization algorithm that finds intersections of grid cells with a strand by means of the *separating axis test*, cf. [6]. For this, we embed each segment of the generalized cylinder (frustum) into an oriented bounding box (OBB). The *separating axis test* is performed for each voxel within the axis aligned bounding box of the frustum and its corresponding OBB.
- **Continuous Density model (CDM)**: For the second model we compute a scalar density field $\Phi_\rho : \mathbb{R}^3 \mapsto \mathbb{R}$ on a rectilinear grid. For each fiber we calculate the fiber-voxel intersections using a voxel traversal algorithm. The local density is increased by the ratio of the segment length inside a cell and the cell diagonal. The idea is to force the fibers into the direction of equal density. For this, the density gradient $\nabla\Phi_\rho$ is computed along the guide curve. The corresponding term added to the objective function writes

  $$\mathcal{F}_4^{CDM} = c_\rho \cdot \int_0^L \left\langle \nabla\Phi_\rho, \frac{\mathbf{r}'}{|\mathbf{r}'|} \right\rangle^2 \mathrm{d}s. \tag{11}$$

  That is, if the direction of the local tangent is parallel to the gradient we add a surcharge of $c_\rho \cdot |\nabla\Phi_\rho|^2$ to the energy value. If the tangent is perpendicular the surcharge is 0 because the fiber's local direction is in optimal alignment with the direction of equal density.
  The gradient of the density field can conveniently be approximated by a central finite difference scheme.

In order to evaluate the degree of homogeneity before and after the incorporation of the density function we computed a density histogram which can be seen in the results section.

3.6 Final Cutting and Strand Interpolation

To generate the full hairstyle from the set of principal guides we employ a simple strand generator. Grouping hairs can be justified by the observation that real hairs tend to form clusters. In a pre-processing step we cut hairs that penetrate the boundaries. This occurs predominantly in the occipital region where the distance from the pore to the boundary is very short. We use our distance field approach to search for the first segment that penetrates the hair volume. If the length of the fiber outside the volume exceeds a predefined threshold before the fiber immerses into the volume again it is cut at the first boundary penetrating segment.

Given the shape of a principal guide we generate a bunch of fibers within a cylindrical region around it. This region is formed by a generalized cylinder with varying radius along the curve. Our scheme is very similar to that of [4] but allows the fibers of a strand to wind around the corresponding guide.

4 Results

For demonstrating the efficiency of our algorithm we generated two hairstyles from two different hair volume surfaces using varying parameter sets. Specifically, we used the following two test cases:

a) a spheroidal volume obtained from a sculpture scan, and
b) a straight hair volume taken from Poser,

cf. Fig. 2. Both generated styles cover one half of a human head model. The results from different perspectives as well as the corresponding visual hull are depicted in Fig. 3. For hair rendering we used the model proposed by Zinke et al. [18]. The respective number of fibers was 90 000 for the first model and 60 000 for the second model. The number of guides used to sample the main flow directions was 3000. The times for hairstyle generation was approximately 1.5 minutes on a Pentium IV (2.2 GHz). As can bee seen in Fig. 3 the results show that our algorithm is capable of preserving all the structural details dictated by the hair volume surface. Empty regions inside the hair volume are caused by insufficient hair lengths, a problem that will be addressed in our future work.

The impact of the two density models CDM and BOM (cf. Sect. 3.5) on the final result with varying values for the weighting parameters are shown in Fig. 4. As can be seen on those examples the hairstyles become stringier with increasing fraction. Furthermore, the distribution of the occupied voxels is more homogeneous with the CDM or BOM than without the density models, cf. Fig. 5 and Fig. 6.

5 Conclusion and Future Work

We have presented a new approach for automated hairstyle generation from raw surface data obtained from sculpture scans. This model can be used to generate initial values for a subsequent physics based hair simulation. However, there are still open questions, e.g., how the hair lengths and main

Fig. 2. The reference hair volume surfaces used to demonstrate the capabilities of our approach. *Left pair*: spheroidal volume and the reconstructed hairstyle. *Right pair*: straight volume and the reconstructed hairstyle.

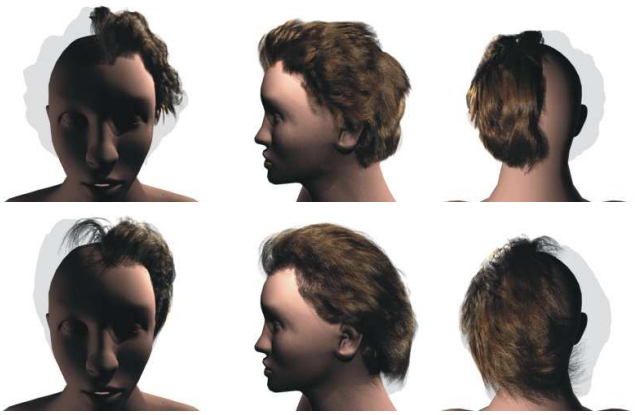

Fig. 3. Overlay of the visual hull of the hair surface and the corresponding hairstyles from different perspectives. Please note the structure preserving capabilities of our algorithm. Empty volume is caused by insufficient hair lengths.

Fig. 4. Same hairstyle with varying contribution of the CDM. Increasing the contribution of the density controlling term results in a stringier look.

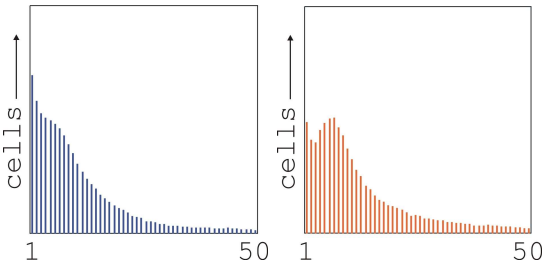

Fig. 5. Histogram of the density distribution. *Left*: Number of segments (1-50) per cell (abscissa) and the number of cells (ordinate) obtained with the CDM. *Right*: The same, but without any density model.

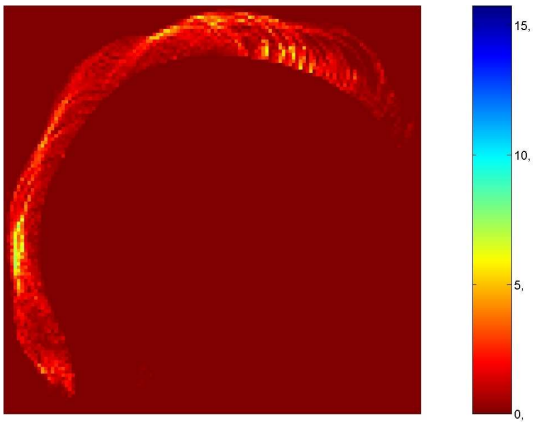

Fig. 6. The picture shows the hair density distribution inside the hair volume (center sagittal plane) obtained with the continuous density model (CDM). Note that the hair density is a) homogeneous and b) zero inside the head.

flow directions can directly be estimated from the hair volume surface in order to further reduce the parameters that must be handled by the user. Addressing these open questions will be the content of future work.

6 Acknowledgements

We are grateful to A. Zinke for many helpful discussions and his assistance in rendering the results. The presented work is partially supported by *Deutsche Forschungsgemeinschaft* under grant We 1945/3-2.

References

[1] Stuart S. Antman. *Nonlinear Problems of Elasticity*, volume 107 of *Appl. Math. Sci.* Springer-Verlag, Berlin and New York, 1995.

[2] Volker Blanz and Thomas Vetter. A morphable model for the synthesis of 3D faces. In *Siggraph 1999, Computer Graphics Proceedings*, pages 187–194, 1999.

[3] David E. Breen, Sean Mauch, Ross T. Whitaker, and Jia Mao. 3D Metamorphosis between different types of geometric models. *Eurographics 2001 Proceedings*, 20(3):36–48, 2001.

[4] Byoungwon Choe and Hyeong-Seok Ko. A statistical wisp model and pseudophysical approaches for interactive hairstyle generation. *IEEE Transactions on Visualization and Computer Graphics*, 11(2):160–170, 2005.

[5] Michael S. Floater. Parametrization and smooth approximation of surface triangulations. *Computer Aided Geometric Design*, 14(4):231–250, 1997.

[6] S. Gottschalk, M. C. Lin, and D. Manocha. OBBTree: A hierarchical structure for rapid interference detection. In *Proceedings of the 23rd annual conference on Computer graphics and interactive techniques*, pages 171–180, 1996.

[7] Sunil Hadap and Nadia Magnenat-Thalmann. Interactive hair styler based on fluid flow. In *Computer Animation and Simulation*, pages 87–100, August 2000.

[8] Ali Haider and Toyohisa Kaneko. Hair shape modeling from video captured images and CT data. In *The Proceedings of ICAT2000*, pages 52–57, 2000.

[9] Tae-Yong Kim and Ulrich Neumann. Interactive multiresolution hair modeling and editing. In *ACM Transactions on Graphics (TOG)*, volume 21(3), pages 620–629, July 2002.

[10] Chai-Ying Lee, Wei-Ru Chen, Eugenia Leu, and Ming Ouhyoung. A rotor platform assisted system for 3d hairstyles. In *(WSCG'2002) - the 10-th International Conference in Central Europe on Computer Graphics, Visualization and Computer Vision'2002*, 2002. To appear.

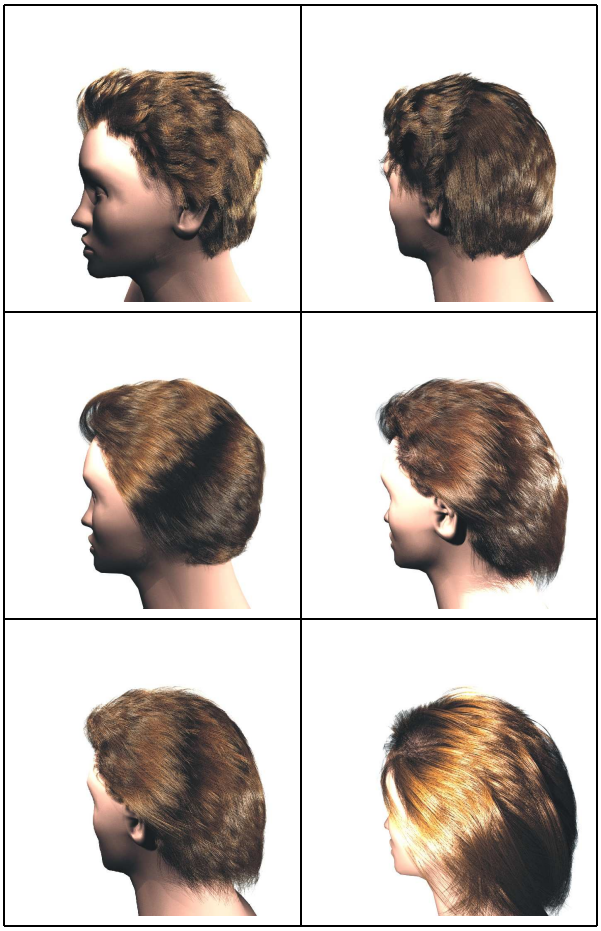

Fig. 7. Hairstyle examples generated with our approach shown from different perspectives. 1) and 2): Hairstyle obtained with the spheroidal hair volume surface. 3): This model was obtained with an increased weighting parameter for the similarity term and a greater hair length. This results in a very smooth look. 4) and 5): Hairstyle obtained with the straight hair volume surface. 6): This model results from increased hair lengths.

[11] Shu Liu and Andreas Weber. A symbolic-numeric method for solving boundary value problems of Kirchhoff rods. In Victor G. Ganzha, Ernst W. Mayr, and Evgenii V. Vorozhtsov, editors, *Computer Algebra in Scientific Computing (CASC '05)*, volume 3718 of *Lecture Notes in Computer Science*, pages 387–398, Kalamata, Greece, September 2005. Springer-Verlag.

[12] Dinesh K. Pai. STRANDS: Interactive simulation of thin solids using Cosserat models. In *Computer Graphics Forum*, volume 21(3), pages 347–352, 2002.

[13] Sylvain Paris, Hector Briceño, and François Sillion. Capture of hair geometry from multiple images. *ACM Transactions on Graphics (Proceedings of the SIGGRAPH conference)*, 2004.

[14] Gerrit Sobottka and Andreas Weber. Computing static electricity on human hair. In *Proceedings of Theory and Practice of Computer Graphics 2006*, 2006.

[15] Yichen Wei, Eyal Ofek, Long Quan, and Heung-Yeung Shum. Modeling hair from multiple views. In *ACM Transactions on Graphics (TOG), 2004*, volume 24(3), pages 816–820, 2005.

[16] Zhan Xu and Xue Dong Yang. V-HairStudio: An interactive tool for hair design. *IEEE Computer Graphics and Application*, 21(3):36–43, May/June 2001.

[17] Yizhou Yu. Modeling realistic virtual hairstyles. In *Proceedings of Pacific Graphics*, pages 295–301, 2001.

[18] Arno Zinke, Gerrit Sobottka, and Andreas Weber. Photo-realistic rendering of blond hair. In *Vision, Modeling, and Visualization (VMV) 2004*, volume 24(3), pages 191–198, 2004.